INFLUENCES OF THE OPERATING PARAMETERS OF EMBROIDERY STITCHES ON ELECTRICAL PROPERTIES OF THE CONDUCTIVE THREADS

Amal Abdullah Albishri[1], Emad El-Din Sayed Gohar[1] and Marwa Mohamed Tharwat[2]

[1]*Faculty of Human Sciences and Designs, Department of Fashion & Textile, King Abdul-Aziz University, Jeddah, Saudi Arabia*
[2]*Faculty of Engineering, Department Electrical and Computer Engineering, King Abdul-Aziz University, Jeddah, Saudi Arabia*
aaalbeshri@uj.edu.sa, egohar@kau.edu.sa, mmzahran1@kau.edu.sa

Abstract: *The conductive threads are very crucial and essential parts of smart textiles. However, there is still a lack of information in general about the operating parameters of embroidery with conductive threads and their influences on communication among electronic components in the e-textiles product. In this article, silver-coated conductive threads have been usage in the fabrication of 4 embroidered designs with two different stitch types (Tatami, Running) and two lengths for each stitch (4 mm, 6 mm). The electrical characteristics were measured and determined in the frequency domain from 100 kHz to 120 MHz. The impedance and resistivity of threads are determined also using the AC voltages at three different frequencies 100 kHz, 1 MHz and 10 MHz. The applied voltages were 0.0 -1.0 volts through thirty (30) steps. The most important results are summarized in the polarization of silver, which is contributing to the measured impedance values so that all stitch types with different lengths have the same behavior and trend. The designs of shapes by embroidered stitches are acting as perfect resistor at low frequencies while they are acting as perfect inductor at high frequencies. The 6 mm stitches length in all stitch types provides low resistance rather than 4 mm stitches against the common prediction. Therefore, these designs of embroidered shapes by certain stitches could be a good potential for antenna applications.*

Keywords: *conductive thread, e-textiles, wearable electronics, embroidery.*

1 INTRODUCTION

Textiles have been developed significantly in recent years than they were in the past, and it has a tendency to take advantage of advanced digital technologies. Therefore, the possible incorporation of electronics has rendered garments a new type of high-tech product [1]. The incorporation of technology into textile during production of smart garments is extremely important as this process involves the integration of two important components, namely textile and electronic units. The incorporation method depends on a desired function as each of many functions has unique requirements that must be met during the incorporation process. Accordingly, smart textile is a broad interdisciplinary field of research that combines design with textile techniques, electrical engineering, and information and communication technology in order to develop new products that meet specific aesthetic, functional and technical requirements [2] in an integrated manner. The incorporation of electronics into textiles has already opened the way for the production of garments with special capabilities which are used in the fields of defense, sports, medicine and health

monitoring [3]. Such an innovation has become supportive of the functions that users aspire to, thus providing greater efficiency to perform the required tasks.

Currently, there are several distinct methods ensuring an effective functional link between textiles and electronics by incorporating conductive threads into fabrics, dyes, painting and embroidery. These methods and their end-use specific functions offer solutions to effectively use the materials with manufacture technology. The function of a textile is determined by the method used for the linking process [4]. This research deals with the technique of embroidery; a traditional method of incorporating threads into fabric, originally used for adding an aesthetic aspect [5] on all kinds of fabrics, given the high potential of embroidery, its rapid adaptation to new designs, and ability to continuously develop [6]. In addition, embroidery is applied on fabrics at the final manufacturing stage, and this can be an advantage because it makes initial manufacturing processes much easier [7, 8] and means for the mass production of electronic textiles [5, 9]. Thus, the ability of embroidery to incorporate electronics into traditional fabrics represents

an opportunity to create new and versatile functions. This is applicable as the integration of multiple sensors and signal processing units to obtain interactive wearable textile systems, enabling the collection of large amounts of information, while providing greater security to the user [10].

Digital embroidery designs also allow the integration of electronic components [wires, switches, sensors or other electronics) into the surface of fabric, and through the use of conductive threads along with or without traditional threads to achieve the electrical conductivity advantage on textiles [11]. Thus, embroidery techniques using conductive threads on substrate fabrics have become a very attractive approach for fabricating textile-based circuits for smart wearables because of their circuit design freedom and ease of manufacture compared to other processes such as weaving, knitting and printing [8]. Automated embroidery has been one of the most widely used fabrication techniques in the field of smart textiles that contributes to the development of flexible and wearable electronics and is therefore referred to most often as electronic embroidery [2].

Electronic embroidery is one of the manufacturing techniques used in the field of smart textiles. In their pioneering work [12] Maggie Orth is responsible for the term e-embroidery, which describes the digital stitching of electro-conductive threads into textiles [13]. She used embroidery to create conductive electrodes for capacitive sensing, inspiring other works and thereby casting the seed for the prospective field of smart textiles [5]. Therefore, embroidered electronic systems are being increasingly researched, leading many researchers to examine the potentials and functional solutions offered by electronic embroidery, including physiological monitoring, due to the potential to place the base material in all directions instead of tailored fiber placement (TFP), including through availing direct contact between electrical sensors and the skin [14, 15], measuring temperature and the ECG signal, use of Electrocardiography (EKG) shirt with embroidered electrodes for measuring an electrocardiogram [16]; use of sensor for measuring an electromyogram [17].

Other researchers examined some medical cases, including the embroidered electrodes and their use in wearable surface electromyography (sEMG) [18]. Meanwhile, Linz et al. presented the first successful measurements with sensors. To obtain maximum unobtrusiveness with sensors for monitoring health parameters on the human body, they combined two technical solutions. First, contactless sensors for capacitive electromyography measurements were proposed. Secondly, the sensors were integrated into textile, so complete fusion with a wearable garment is enabled [19]. Roh et al. introduced the all-fabric intelligent temperature regulation system for smart clothing applications [20].

The techniques used in electronic embroidery to date can be identified in single-thread embroidery (ring stitches) which have been used mostly in body signal measurements. Two-thread embroidery (standard embroidery) which is a very versatile method for creating new technical materials that rely on precision and are repeatable. Intricate patterns can be achieved, such as circuit board stitching, pinch gesture recognition, strain and deformation sensors (resistive or capacitive sensors), moisture sensors (either capacitive or short- circuit based) [6, 9]. However, tailored fiber placement (TFP) places high tenacity fibers on a basic fabric to create preforms. TFP allows the exact placement of fiber and fiber - like materials onto a textile substrate. Electrically conductive yarns offer a variety of braiding possibilities [2, 9]. Each technique is used separately and the techniques can be combined according to the functional purpose.

In the field of communication and data transmission technology, automated embroidery using conductive threaded is considered a promising technique as antennas can be incorporated into garments [21-24]. With the continued increase in demand for smart wearable fabric systems, many studies have dealt with modeling embroidered contacts for electronics in textiles [25] as well as with employing embroidery inductors to increase the success of a textile-based circuit [26] and employing embroidery in a simple and easy manufacturing technique aimed at creating robust, reliable, pressure-sensitive sensors for concrete and wearable interfaces. The textile-based sensor technology is also an important component of textile industry, as it provides potential for incorporation into woven fabrics [27]. Other studies have examined the use of embroidered textile-based pressure sensors [5, 28-32]. The joining of conductive threads through embroidery was not limited to previous functions, but it included also the creation of an electronic chip board using conductive threads, incorporating framed-electronic components into fabric [33] and interaction-centered applications, such as pinch gesture recognition on textiles [34]. In general, there is lack of information about the operating parameters of embroidery with conductive threads and their influences on communication among electronic components in the e-textiles product. Some of these parameters are length of stiches, type of the stiches, type of conductive materials and conductive threads, electrical properties of those conductive threads and the communication of signals flow in the possible contacts of the conductive thread. In this article, a comparison study between two types of stitches made within different length and different conductive thread with a same conductive material as silver was made. The conductive thread and threads are very crucial and essential parts of the smart textiles. The variations in the application of silver-coated

synthetic (polyamide, polyester and nylon) threads beside natural (cotton, silk and wool) threads in embroidery are very wide the electrical properties and characteristics must be well studied and known for each specific and proper application.

2 MATERIALS AND METHODS

The appropriate commercial conductive threads Amman silver tech-50 and Madeira HC12 have been selected for embroidery, also obtaining standard 100BY OEKO-TEX. We have been provided with standard threads by the company.

Table 1 Standard threads

Threads type		A (silver tech-50)	B (HC12)
Threads size [count] [35]	Tex no	62	62
	Linear density [dtex]	210*3	616*2
Threads diameter [35]	Optical diameter [mm]	0.36	0.39
Tensile properties of threads [36]	Breaking force [cN]	1930	2950
	Elongation at break [%]	20	22

The conductive threads A and B have been employed in fabrication of 4 embroidered designs with two different stitches types (Tatami, Running) and two lengths for each stitch type (4 mm, 6 mm). The basic textile of military camouflage was used for the Kingdom of Saudi Arabia and two layers of supportive textile were used for embroidery of Vaseline to reinforce the fabric on the back to prevent damage and tear in delicate materials and as a backing and reinforcing layer for embroidery. Based on the previous variables, the following design was proposed to implement embroidery samples in a way that suits the possibility of taking electrical measurements, as it requires preparing the design with a length of 1 meter and a spacing of 3 mm for the Running stitch and as for the samples of stitches (Tatami stitch) area of 5x5 cm and at an angle of 90°.

Embroidery samples were performed using an ELUCKY embroidery machine with an 11/75 needle to fit the thickness of the fabric. The morphological structure and texture of the conductive fibers spun to the thread were studied and measured in terms of dimensions and components the scanning electron microscope SEM, Quanta FEG 250, FEI and equipped with energy

dispersion of X-ray spectroscopy technique EDX, Dutch company Quanta with field emission with an electric voltage of 5 kV to 30 kV. The Polarizing optical microscopy POM using Leica DM750P (Leica Microsystems, Switzerland) equipped with reflection Kit was used to investigate the texture of thread and their coating layer. The electrical properties of the conductive threads were measured and determined by the electrical characteristics using AC High Tester 3535 (Hioki, Japan) in frequency domain from 100 KHz to 120 MHz for high range of frequencies. While the lower range was measured by Ando AG-4311B LCR meter.
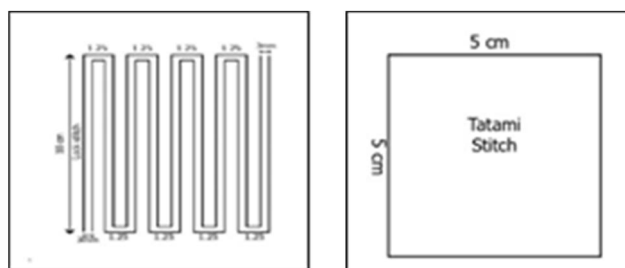
Figure 1 Design of embroidery samples

3 RESULTS AND DISCUSSION

3.1 Thickness of threads

There are discrepancies in the thickness for the two types of the conductive threads, where are determined from scanning electron microscope as well as polarizing optical microscope as stated in morphology sections. The thicknesses are shown in Table 2, because the thickness of those conductive threads is a vital parameter in the electrical properties determination.

Table 2 Thickness of threads by both SEM and POM techniques

Threads	Diameter [mm]	Radius [mm]
A	0.35±0.05	0.175±0.025
B	0.50±0.05	0.250±0.025

The following laboratory tests were conducted at the Saudi Standards, Metrology and Quality Organization (SASO) and to determine the specifications of the fabrics used and were as in Table 3.

Table 1 Standard of the fabrics used

Textile	Fiber composition [37]	Weave identification (construction) [38]	Fabric thickness [mm] [39]	Thread per unit length [40]		Fabric tensile strength [N] [41]		Mass per unit area [g/m^2] [42]
				warp	weft	warp	weft	
Basic textile	polyesters and viscose	plain weave 1/1	0.3	32/cm	32/cm	1032.8	822.2	201
Supportive textile	polyesters	non-woven	0.19			70.9*	63.4*	50

*marked testing included in accreditation scope in SASO

3.2 Metal composition of the embroidery threads

The conductive filaments were imaged with a scanning electron microscope technology at different levels of magnification up to 6000x. The fibers spun to the thread were studied and measured in terms of dimensions and components of it by X-ray energy dispersion spectroscopy technique attached to the scanning electron microscope made by the Dutch company Quanta with field emission with an electric voltage from 5 to 30 kV.
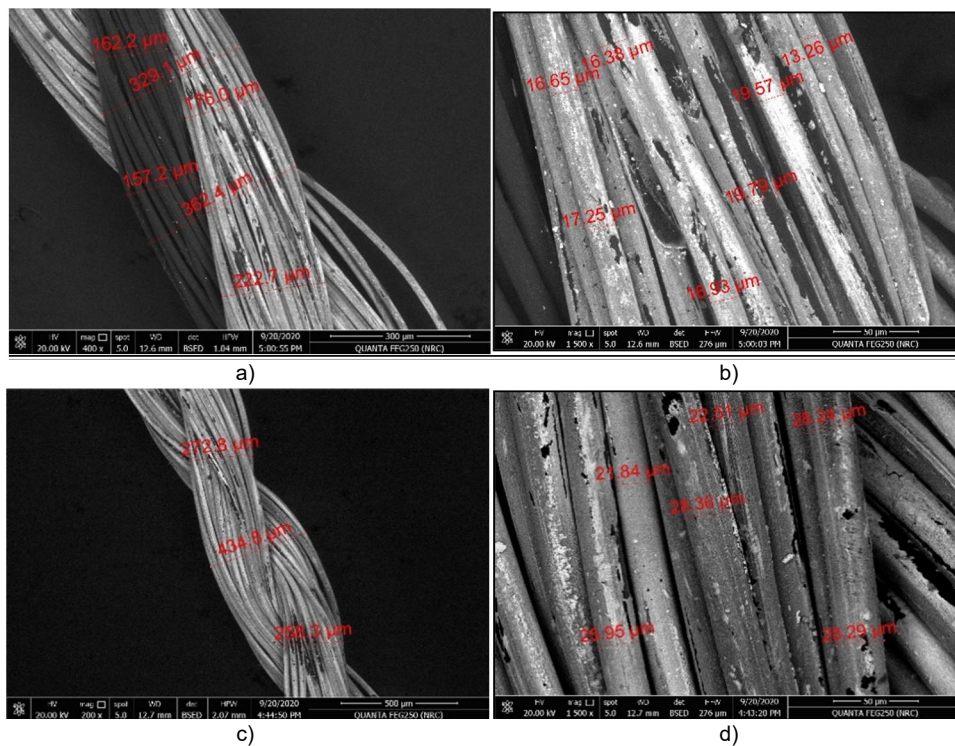
The Figure 3 shows an imaging of thread using a polarized optical microscope.

The X-ray energy dispersive spectroscopy of the threads is given in Figure 4.

Through the above, the basic components that make up the threads can be summarized in the Table 4.

Table 2 the basic components for the threads

Conductive thread	Element [%]		
	C	**O**	**Ag**
A	50.22	33.08	16.69
B	29.10	17.58	53.31

Figure 2 Conductive filament imaging of A thread (a, b) and for B thread (c, d) at different magnifications (a - 400x; b, d - 1500x and c - 200x)

c)   d)
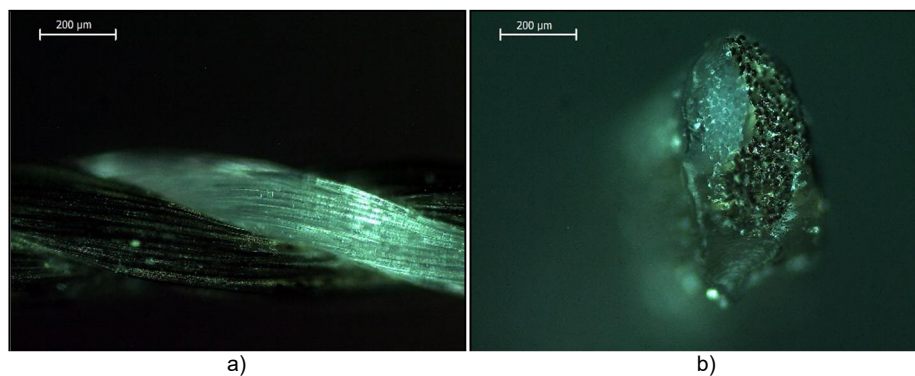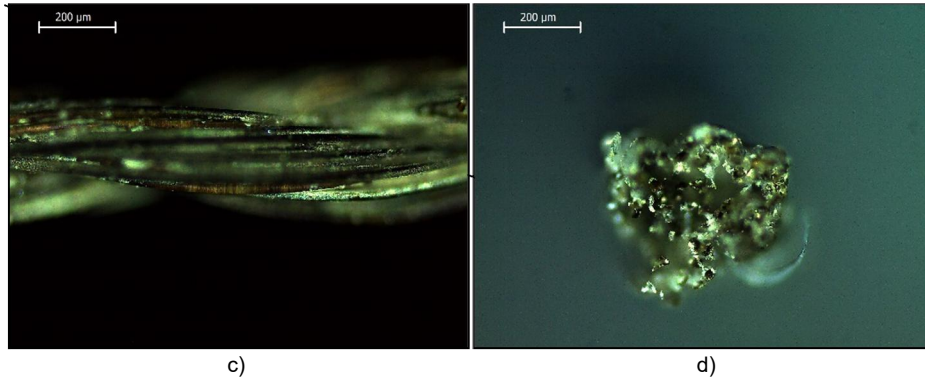
Figure 3 The longitudinal section of the conductive A thread using a polarizing optical microscope with magnification 200x (a), the A thread cross-section (b); the longitudinal section of the conductive B thread (c) with magnification 200x and the B thread cross-section (d)

Lsec: 30.0 0 Cnts 0.000 keV Det: Octane Pro Det   Reso

A thread

Lsec: 30.0   1 Cnts   13.270 keV   Det: Octane Pro
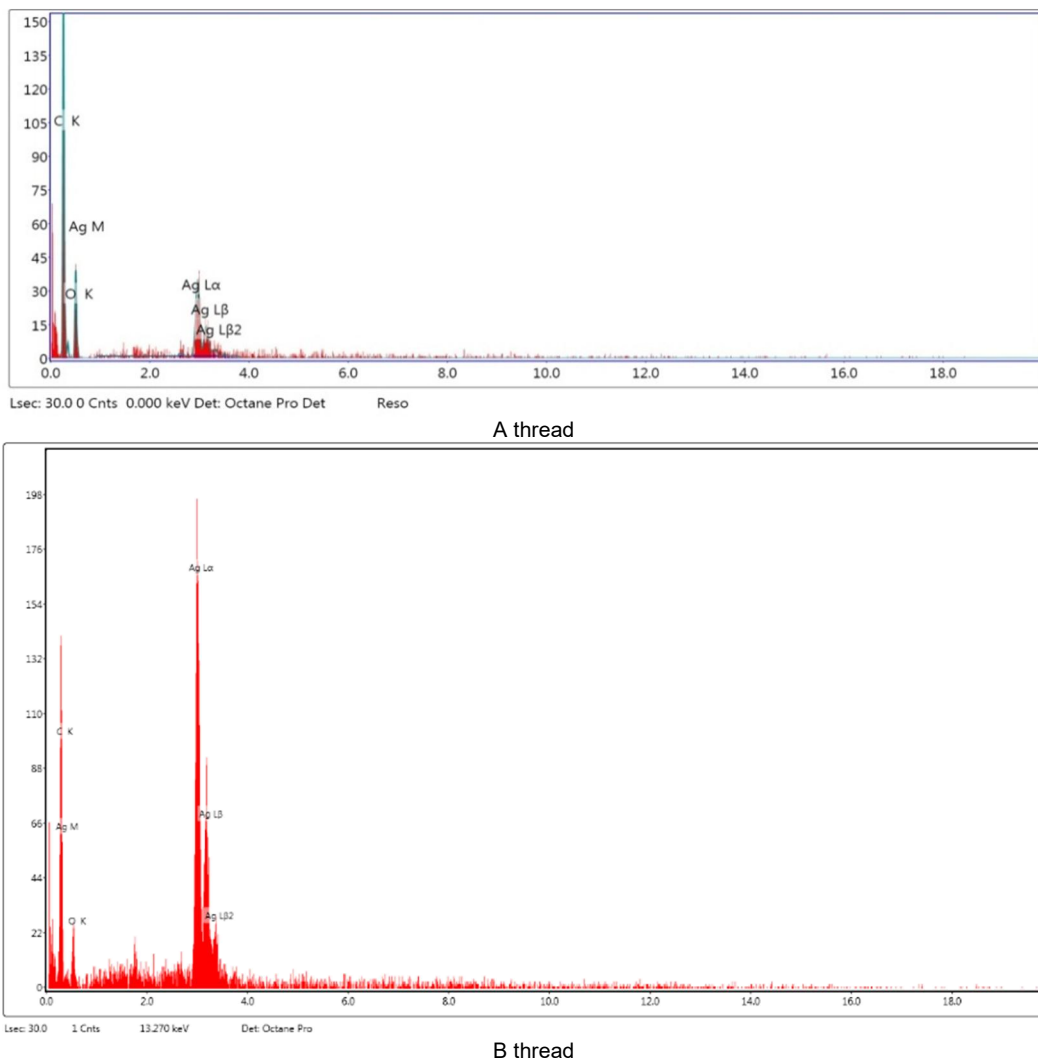
B thread

Figure 4 The X-ray energy dispersive spectroscopy of the threads

3.3 Electrical proprieties

There were having different DEN and other textile parameters as stated in their datasheet. The electrical characteristics were measured and determined using AC High Tester 3535 (Hioki, Japan) in frequency domain from 100 KHz to 120 MHz. This range was carefully selected for futuristic studies on antenna performance and efficiencies of those threads. Moreover, the efficacy of the embroidered conductive thread will be examined within different shapes, length, and designs. The impedance and resistivity of threads are determined also using the AC voltages at three different frequency 100 KHz, 1 MHz and 10 MHz.

The applied voltages are from 0.0-1.0 V through thirty (30) steps. The voltage should be small because the thread performance will be dealing with small voltages and signals from embedded electronics, sensors, and surrounding stimuli. Thus, the electrical test ought to consider these variations in the measurements of any electrical properties or parameters. These voltages were applied at 3 different frequencies: 100 KHz, 1.0 MHz and 10 MHz.

Electrical resistivity ρ [Ω.m] is known as specific electrical resistance or volume resistivity, which is an intrinsic property of matter. Electrical resistivity determines how strongly conductive thread resists or conducts electric current. Thus, low material resistivity means high conducting materials that allow electric current [42].

The A thread resistivity is a little bit lower than former conductive threads. Where, it was stable at 1.63 Ω.cm and 1.78 Ω.cm with 0.1 and 1.0 MHz respectively. Within 230% increase of resistivity, the A thread became 3.77 Ω·cm at 10 MHz for all applied voltages (see Fig.5-a).

In Fig.5-b), the resistivity of B conductive thread is stable at 2.27 Ω·cm and 2.22 Ω·cm with different voltages at 0.1 and 1.0 MHz respectively. While at 10 MHz the resistivity increased to 4.39 Ω.cm, but it was steady with all applied voltages.

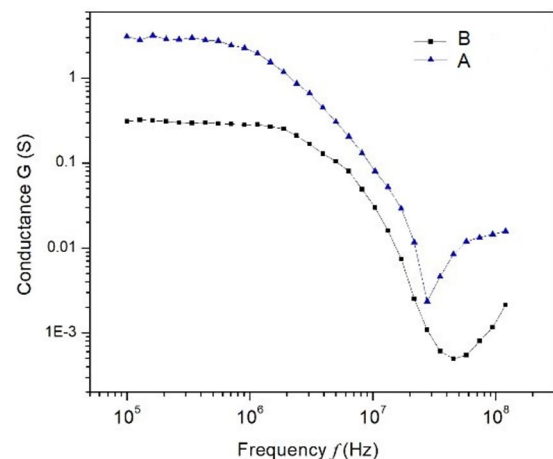_Conductance G [S]_

The reciprocal quantity of electrical resistance which is a measure opposition to the electric current flow for an object is the electrical conductance. Thus, electrical conductance is a measure for an electric current to pass through an object easily. According to Ohm's law, both current I and potential V are proportional to each other, the constant of this proportionality is resistance R or conductance G [43].

$$R = \frac{V}{I}, \qquad G = \frac{I}{V} = \frac{1}{R} \tag{1}$$
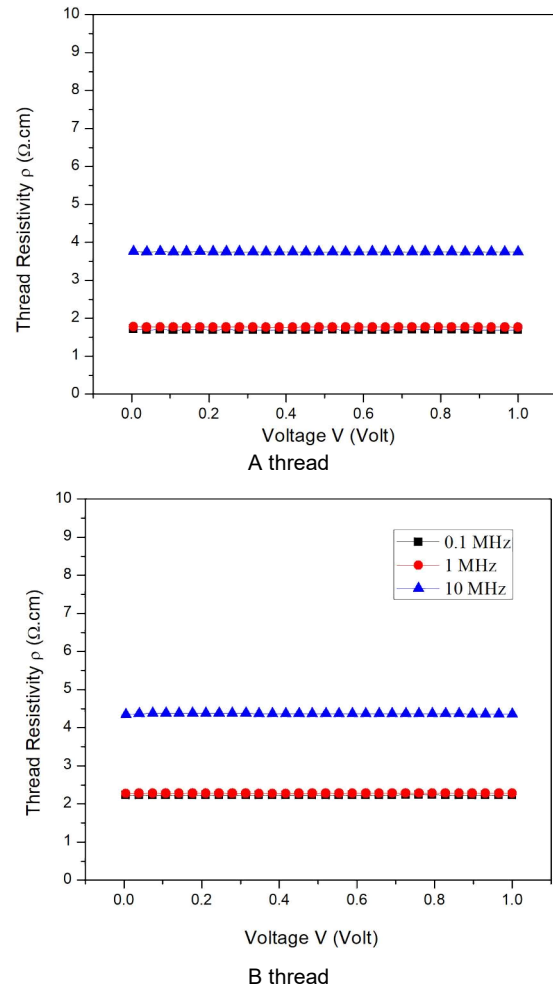
Figure 5 The electrical resistivity of threads measured with different voltages in range of 0.0-1.0 V at three different frequencies 100 KHz, 1.0 MHz and 10 MHz
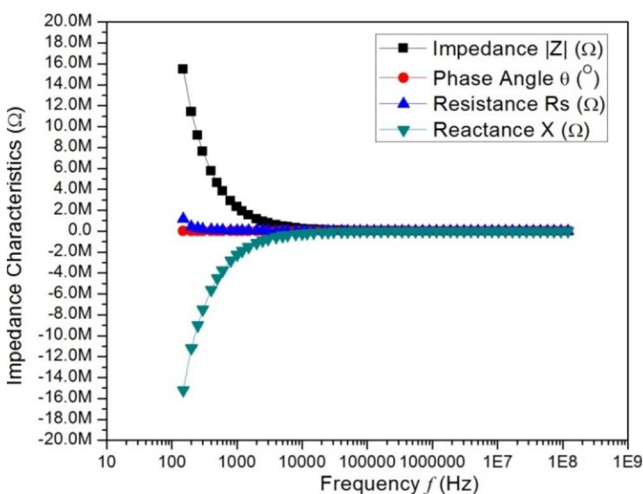

Figure 6 Log-Log scale graph of the thread electrical conductance G for all conductive threads against the frequencies

In Figure 6, the electrical conductance G is the highest for both A and B thread around 4 S. Several factors could affect electrical conductance such as the quality of coating, the thickness of conductive threads, length of threads and the composition of threads (as stated in morphology sections) [44-46]. It was worthy to be noted the conductance stability against frequencies is variant from each thread to another. A and B threads show the lowest stability until a few MHz, but having the highest electrical conductance values.

3.4 Electrical properties of embroidered textile

The embroidered textile consists of three layers for summer seasons using light material that designed to the militarily use. The embroidery has been performed using two extra supported textiles for embroidery. The electrical characteristics also have been determined for the textile without any embroidered stitches or conductive threads. In Figure 7, the impedance |Z| is typical of insulator material in range 15.5 MΩ at 150 Hz and decreased exponentially to 23.5 KΩ at 100 KHz. Then at high frequencies, the |Z| is reach to 177 Ω at 120 MHz. The phase angle is stable against all frequencies up to 100 MHz at -89° which is the characteristic of good small resistor accompanied with a capacitor. The reason for that is the textile in between parallel two electrodes acting as typical dielectric material. The real part of Z^* as the resistance Rs is decrease exponentially also as |Z| but starting from lower value at 1.15 MΩ at 150 Hz and continue in the decrease to 49 Ω at 120 MHz. the reactance X as imaginary part of Z^* is increased from -15.2 MΩ at 100 Hz and then increased to -170 Ω at 120 MHz in exponential way.

to assess the stability of a system with feedback. In Cartesian coordinates, the real part of the transfer function is plotted on the X axis, and the imaginary part is plotted on the Y axis. The frequency is swept as a parameter, resulting in a plot based on frequency. The Nyquist plot here is typical for insulator component as shown in Figure 8, which the Nyquist plot of blank textile declare the stability of the textile against the frequency which decrease from 1.2 MΩ to the lowest value 177 Ω of impedance at highest frequency 120 MHz.
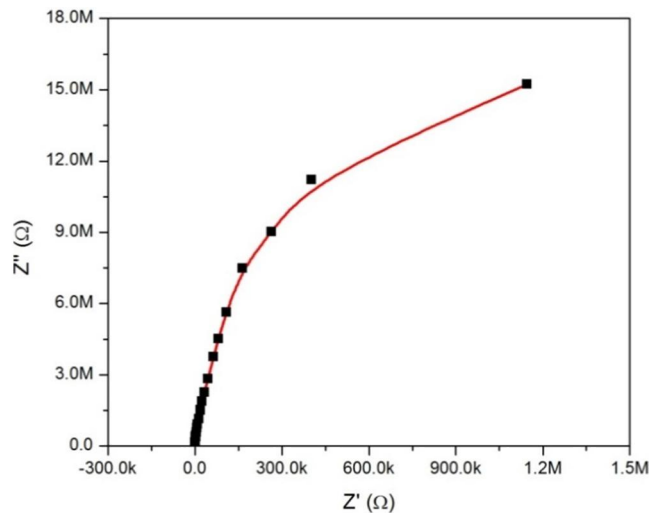
Figure 8 The Nyquist plot based on broad range of the frequencies for different embroidered stitches for E-clothes using Silver tech 50 conductive threads. The experimental real and imaginary values of the impedance of the conductive embroidered stitches in two different lengths
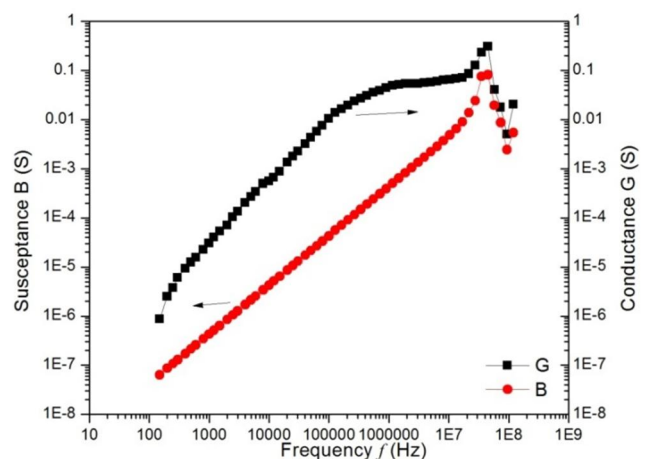

Figure 7 The semi-log scale plot of the impedance |Z| characteristics against the frequencies applied for embroidery on the blank textile without stitches

Figure 9 The conductance G and susceptance B against of the frequencies for E-clothes blank textile without any embroidered stitches. The experimental real G and imaginary B values of the admittance are co-presented

The Nyquist plot (or Nyquist Diagram) is a frequency response plot used in control engineering and signal processing. Nyquist plots are commonly used

In Figure 9, the real and imaginary part of admittance |Y| values G and susceptance B are plotted against the applied frequencies from 100 Hz

to 120 MHz. The current flow is not conducted in blank textile materials. The conductance G is very small which starts at 0.85 µS at 150 Hz and increase exponentially with increasing frequencies up to 0.065 S at 1 MHz then go into plateau for one decade of MHz from 0.8 MHz to 20 MHz. while the susceptance B is much smaller than conductance G. The susceptance B is increased from 62.5 mS at 150 Hz up to 0.014 S at 100 MHz as is shown in Figure 9.

3.5 Embroidery proprieties

The conductive threads A and B have been employed in fabrication of 4 embroidered designs with two different stitches types (Tatami, Running) and two length for each stitch (4 mm, 6 mm), (Table 5).

3.6 Alternative current AC measurements

The conductive thread A and B threads have been employed in fabrication of 4 embroidered designs with two different stitch types (Tatami, Running) and two length for each stitch (4 mm, 6 mm). The impedance against frequencies from 100 Hz-120 MHz is plotted in Log-Log scale that measured for two types of stitches with two different stitch lengths for each stitch type (4 mm and 6 mm).

It is clearly seen from Figure 10a) that for A conductive thread, the impedance of Tatami stitches within length 6 mm has the lowest value at 0.6 Ω and stable from 100 Hz to 0.1 MHz but within 4 mm

length to be 1.3 Ω in average for the same frequencies.

In the B conductive thread, the impedance of Tatami stitches within length 6 mm has the lowest value rather than the same type of stitch but within 4mm in low frequencies from 100 Hz to 1 MHz.
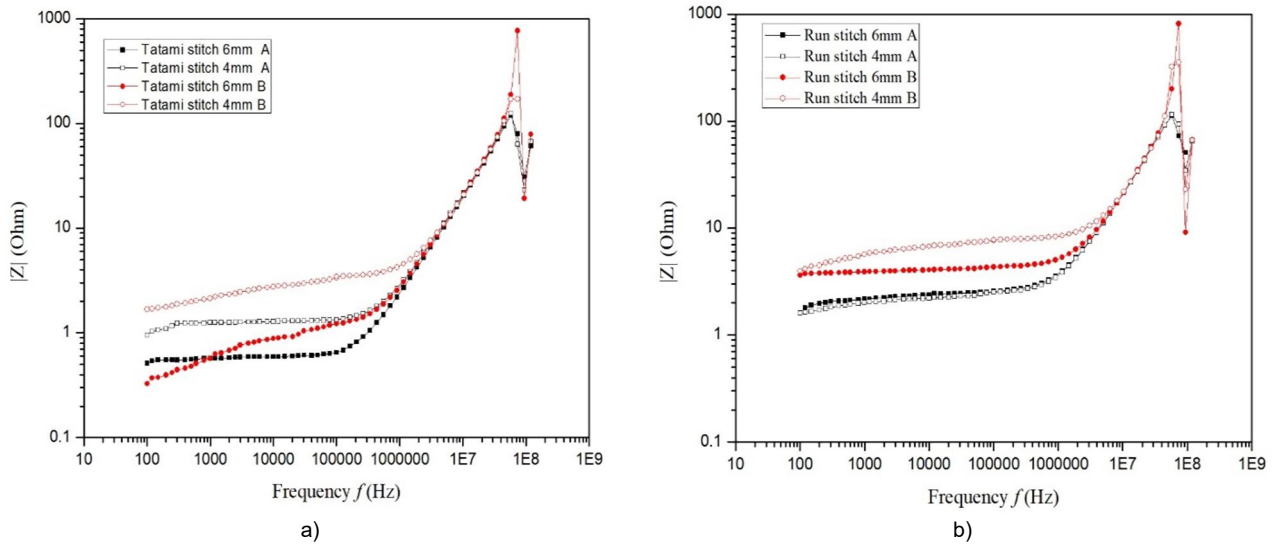
However, the impedance of Running stitch in a conductive thread one for its both length 4 mm and 6 mm are nearly the same and in a gradual increase from 1.6 Ω to 2.98 Ω. All impedance values are located between 0.6 Ω up to 4.3 Ω. Once, the impedance is crossing the frequency of 1 MHz, the polarization of silver is contributing again to the measurement, so that all stitches types with different length have the same behavior and trend, also the impedance becomes too high up to 120 Ω at high frequencies 100 MHz as it is shown in Figure 10b).

The same trend is observed also in the Running type stitches in B conductive thread of 6 mm stitch length against 4 mm stitch length also at low frequency. The Running stitch type of stitches has lower impedance than Tatami ones but is higher than Tatami stitches. All impedance values are located between 0.3 Ω up to 6.18 Ω. Once, the impedance is crossing the frequency of 10 MHz, the polarization of silver is contributing to the measurement so that all stitches types with different lengths have the same behavior and trend as is shown in Figure 10b).

Table 5 Embroidery stitches performance of the different on conductive threads

| Type of stitches	Running stitch		Tatami stitch	
Length of stitch	4 mm	6 mm	4 mm	6 mm
A thread				
B thread				

Figure 10 The absolute value of impedance |*Z*| against the frequencies of different embroidered stitches for E-clothes

In A conductive thread, the phase angle is increased exponentially from very low values near to zero until 1 MHz, then the angle continues increasing into the plateau that started from 1-10 MHz with values near 90°. The same trend as in another B conductive thread is observed in the A conductive thread. However, the design's shapes by embroidered stitches are acting as a perfect resistor at low frequencies while they are acting as a perfect inductor. In A conductive thread Satin stitches within 6 mm length are showing the lowest phase angle. On contrary, the Tatami 6 mm stitches length is the highest phase angle at low frequencies. Phase angles in between Tatami 6 mm, other stitch types have typical trends also which Tatami 4 mm override, as well as both Running stitches of 4 mm and 6 mm, are override on each other. All stitch types override on each other at high frequencies 10-100 MHz.

The impedance phase angle for any component (in our case the embroidered stitches designs) is defined as the phase shift between the voltage across that component and current through that component. For a perfect resistor, the voltage drop and current are always in phase with each other, and so the impedance angle of a resistor is said to be 0°. For a perfect inductor, voltage drop always leads current by 90°, and so an inductor's impedance phase angle is said to be +90°. For a perfect capacitor, voltage drop always lags current by 90°, and so a capacitor's impedance phase angle is said to be -90°. Therefore, the impedances in AC behave analogously to resistances in DC circuits: they add in series, and they diminish in parallel.
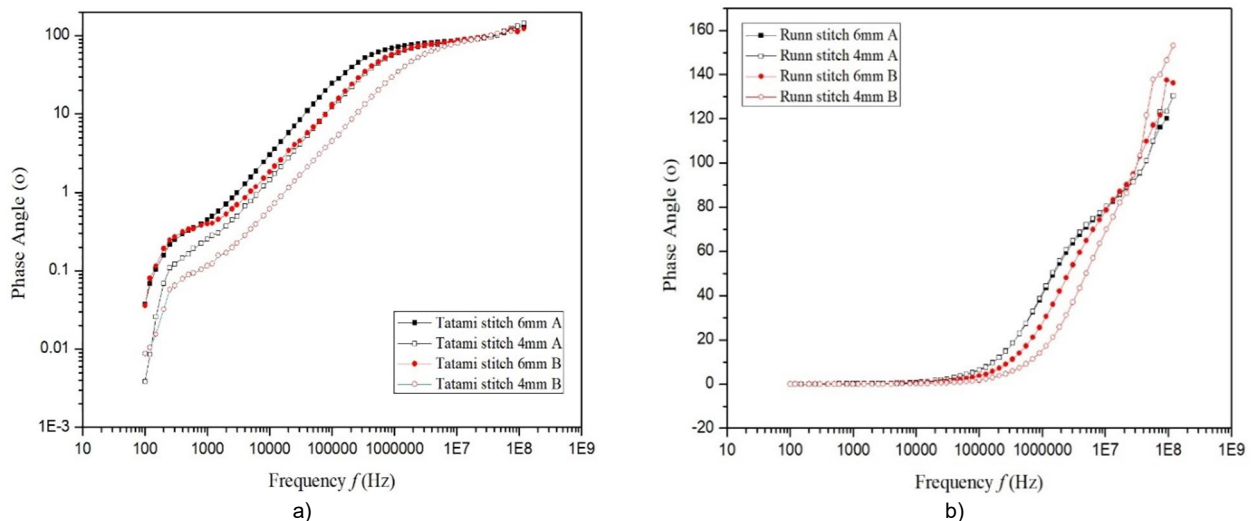
Figure 11 The absolute value of impedance phase angle against the frequencies of different embroidered stitches for E-clothes

In Figure11 the phase angle is increased exponentially from very low values near to zero until 100 KHz, then the angle continues increasing to the plateau that started at 1-10 MHz with values near 90°.

$$R = |Z| \cos \theta \qquad (2)$$
$$X = |Z| \sin \theta \qquad (3)$$

This means the design's shapes by embroidered stitches are acting as a perfect resistor at low frequencies while they are acting as a perfect inductor. Running stitches (B) within 4 mm length are showing the lowest phase angle. On contrary, in the B conductive thread the Tatami 6 mm stitches length is the highest phase angle at low frequencies but the same with Tatami in B thread 4 mm at high frequencies.

The same trend of 6 mm in B thread is observed, which is higher than 4 mm in B thread in all stitches. Thus, the 4 mm in B thread length is favorable for low phase shift designed embroidered stitches electronic component.

In Figure 12, the real value of resistance Rs is shown against the wide range of frequencies from 100 Hz up to 120 MHz. The Rs is real part of the impedance complex Z^* as the following:

$$Z^* = Z' + jZ'' = |Z|e^{j\theta} = R + jX \qquad (4)$$

where: Z' is the real part of the complex impedance, which is represented by resistance value R. Similarly, the imaginary part Z'' is the amount of dissipated energy of the current signal in the circuit component. This term is always represented with $j = \sqrt{-1}$ imaginary symbol [47]. This imaginary part is valued by reactance X.

In Figure 12, the real value of resistance Rs is shown against the wide range of frequencies from 100 Hz up to 120 MHz.

The Rs of 6 mm Tatami stitches in A conductive thread with length 6 mm is the lowest resistance and it is a half value of the 4 mm Tatami stitches. The 6 mm Tatami stitches in A conductive thread is similar to B conductive threads as well.

Also, the resistance of Tatami stitches in B conductive threads with length 6 mm is the lowest resistance and it is in the few-tenth other Tatami stitches with length 4 mm. The 6 mm stitches length in all stitches types provides low resistance rather than 4 mm stitches against the common prediction. This could be explained as the stress and strain due to the automatic machines of embroidery are less in 6mm if compared to these stresses accompanied with 4 mm stitches length.

The reactance X is the imaginary part of the impedance. It is the opposition of a circuit component to the current flow due to the inductance or capacitance of that component. Higher reactance leads to smaller currents at the same voltage applied. Although, reactance X is similar to electric resistance in this respect even if is measuring unit is "ohm" it also but differs in that reactance does not lead to dissipation of electrical energy as heat. Instead, energy is stored in the reactance and later returned to the circuit whereas a resistance continuously loses energy. Therefore, these designs of embroidered shapes by certain stitches could be a good potential for antenna applications. The reactance X is below 1 Ω until 1 MHz, while there is a continuous increase after 1 MHz to 100 Ω till 120 MHz, approximately as well as B conductive thread embroidery. The X is a typical trend without any significant differences in all types of stitches with their different stitch lengths (Figure 13).
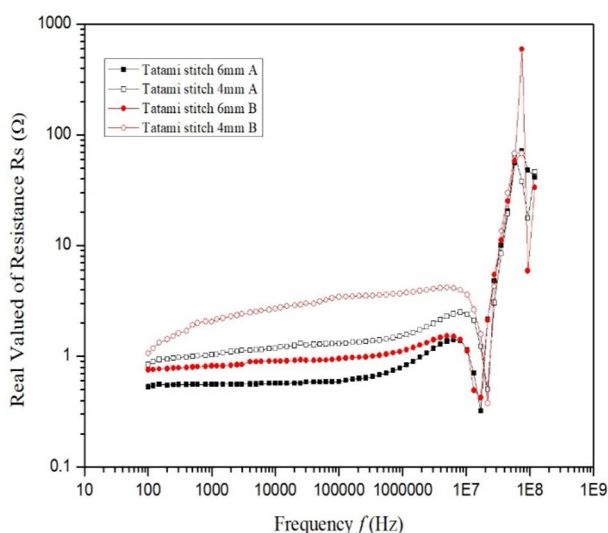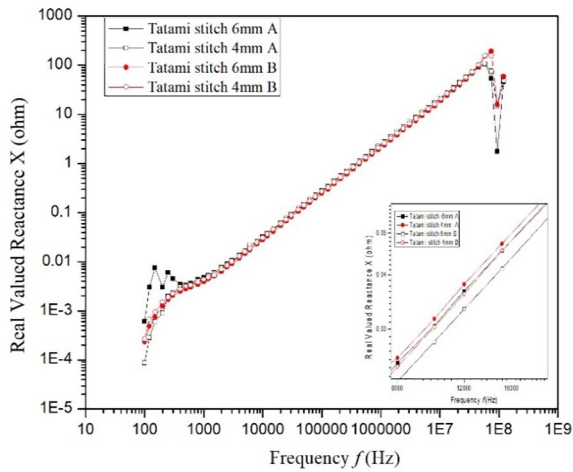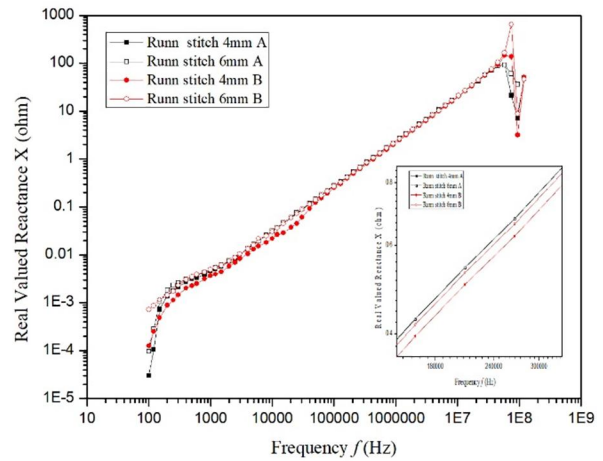

a)
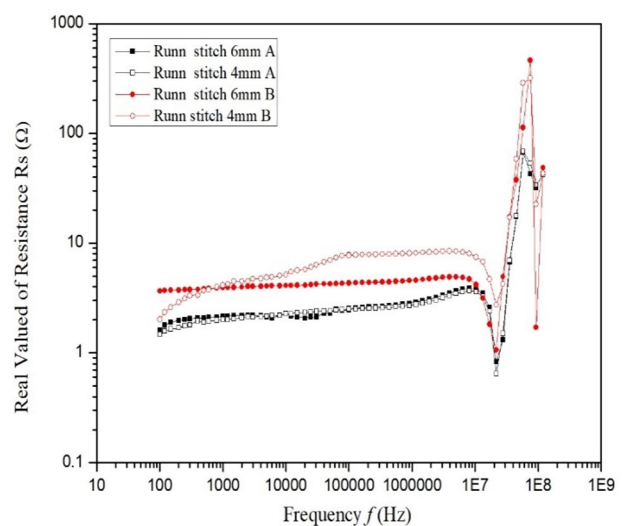
b)

Figure 12 The real value of resistance Rs against the frequencies of different embroidered stitches for E-clothes

Figure 13 The reactance *X* of the designed embroidered shapes by A conductive thread plotted in log-log scale against applied frequencies

However, a much close up to the reactance *X*, one can find that the Tatami 6 mm in A conductive thread is the lowest reactance but Tatami 4 mm is the highest reactance *X*. Both lengths of running stitches have the same values in A conductive thread, also, the reactance *X* of Running stitches 6 mm and 4 mm. One can find that the Tatami 6 mm in B conductive thread is the lowest reactance. Also, the reactance *X* of Running stitches of 4 mm is lower than the 6 mm.

The Nyquist plot (or Nyquist Diagram) is a frequency response plot used in control engineering and signal processing. Nyquist plots are commonly used to assess the stability of a system with feedback [48, 49]. In Cartesian coordinates, the real part of the transfer function is plotted on the X-axis, and the imaginary part is plotted on the Y-axis. The frequency is swept as a parameter, resulting

in a plot based on frequency. The Nyquist plot here is typical for conductive component for all stitches types in both stitches lengths 4 mm and 6 mm. In Figure 14a), the Nyquist plot of A conductive thread is presented. The Tatami stitches length of 6 mm is showing the lowest value of impedance 0.5-0.65 Ω.

In B conductive thread, the Nyquist plot of Tatami stitches length of 6 mm is showing the lowest value of impedance overall the frequencies against the Running stitches 4 mm length in B conductive thread which shows the highest impedance and resistance (Figure 14b). Also, in Figure 14b), the Running stitches of A conductive thread of 4 mm and 6 mm lengths have high values of impedance from 3.5-4.0 Ω but very small reactance near zero across all low frequencies up to a few MHz.
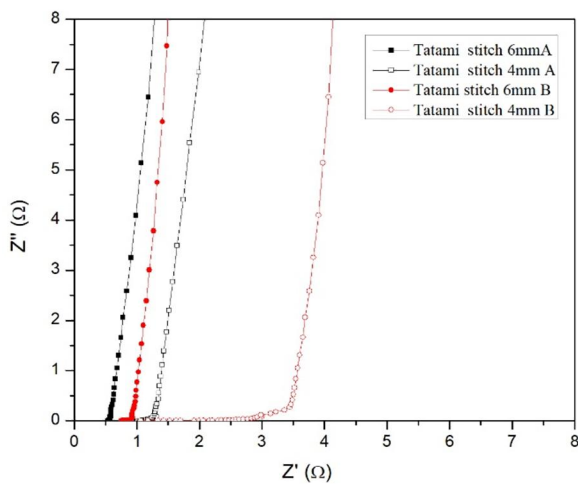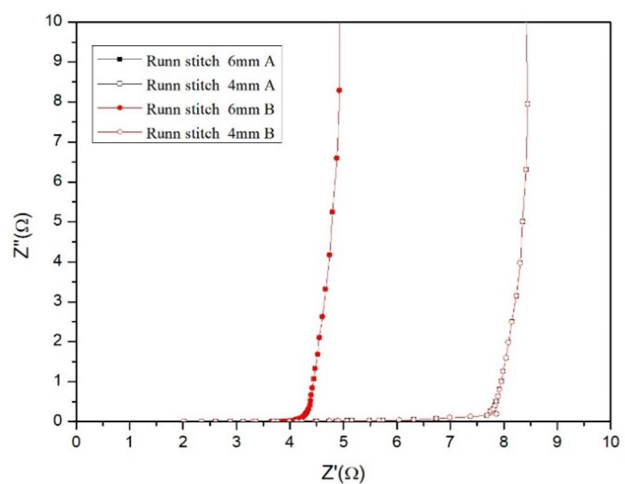
Figure 14 The Nyquist plot based on broad range of the frequencies for different embroidered stitches for E-clothes. The experimental real and imaginary values of the impedance of the conductive embroidered stitches in two different lengths are presented

On the other hand, the admittance $Y = 1/Z$ is reciprocal of the impedance Z, which is a measure of how easily a circuit or device will allow a current to flow. Likewise, the admittance Y is not only a measure of the ease with which a steady current can flow, but also the dynamic effects of the material's susceptance B to polarization. These dynamic effects of the material's susceptance are relating to the universal dielectric response, the power law scaling of a system's admittance with frequency under alternating current AC conditions. The complex admittance Y^* is consisted of the conductance G as a real part while the imaginary part is the susceptance B as the following:

$$Y = G + jB \qquad (5)$$

where: Y, G and B are measured in Siemens [S].

In Figure 15a), the absolute admittance $|Y|$ values are plotted against the applied frequencies from 100 Hz-120 MHz. The current flow is easily conduced in designed embroidered stitches by Tatami stitches in B conductive thread as the length parameter 6 mm very easy starting from 3 S to 0.8 S along with frequencies up to 800 kHz.

In Figure 15a), the absolute admittance $|Y|$ values are plotted against the applied frequencies from 100 Hz - 120 MHz. The current flow is easily conducted in the designed embroidered stitches by Tatami stitches in A conductive thread within length parameter 6 mm as the highest value of the admittance as stable from 1.79-1.58 S in frequency range 100 Hz - 200 KHz, then the admittance decrease rapidly to 0.02 S at 100 MHz. On the opposite, for the same stitches type of Tatami but with stitches l; length 4 mm, the $|Y|$ is the smallest value, and the opponent to current flow is much higher than other stitches.

The $|Y|$ is 0.46 S at 100 Hz and slightly declined to 0.207 S but at a much higher frequency (1 MHz) than other stitches types. Thus, the stability against the frequencies is increased on the count of the admittance value. Then, Satin stitches 4 mm have lower admittance than Tatami 6 mm. After that, the $|Y|$ of Tatami 4 mm has continued the decrease and Running stitches in A conductive thread in both 4 mm and 6 mm are located at 0.46 S in Figure 15b). However, the stability of the admittance against the high frequency is in favor of the Running stitches rather than other types of stitches.

In final the lowest admittance lower than 0.3 S, the Running stitches in B conductive thread with both length 6 mm and then 4 mm Running stitches are ordered (Figure 15b).

Therefore, the real G and imaginary B component of the complex admittance Y^* is illustrated in the Figures 16 and 17. In the Figure 16, the conductance G is behaving as similar as the admittance but in different values and stability against the frequency up to 30 MHz.

All conductance values of stitches types and lengths located in between 0.35-2.0 S approximately all over the measured frequency range. Then, the instability in the conductance after 30 MHz is due to the resonance of the silver metal that is coating the polymeric thread and filament as well as B conductive thread as the experimental limitations.

Whereas, in Figure 16., the imaginary part B which is representing the susceptance B of the materials (silvery conductive threads) in embroidered designed shapes by different types of stitches as Tatami, Satin and Running multiplied within two different lengths 4 mm and 6 mm. The susceptance B is related to the impedance Z and reactance X of the materials as shown before in equation (6).

a)   b)
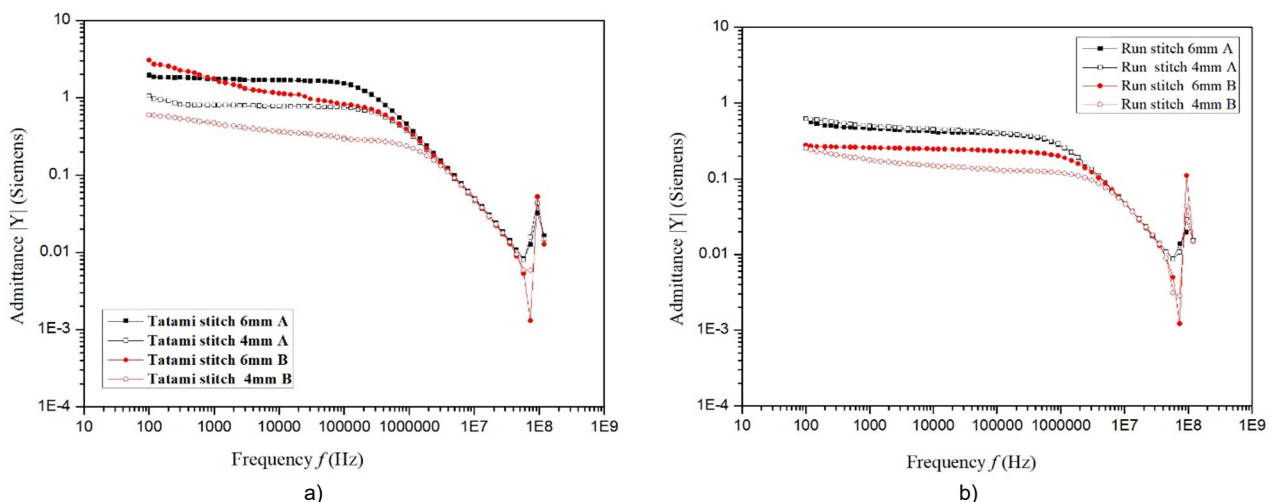
Figure 15 The log-log scale plot of the admittance Y against the frequencies for different embroidered stitches for E-clothes
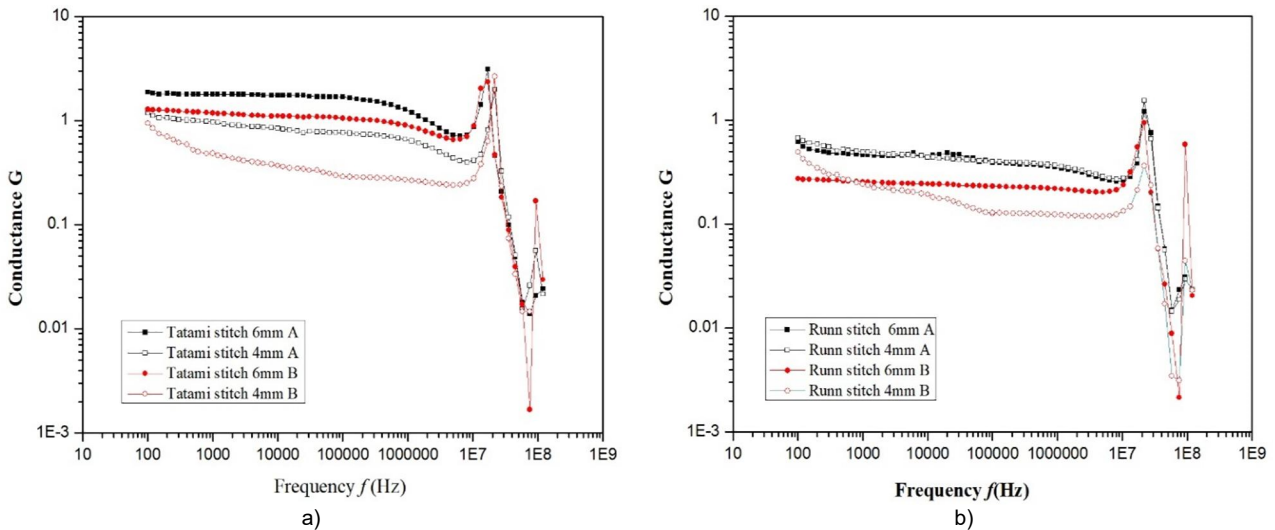
Figure 16 The log-log scale plot of the real part of admittance *Y* as the conductance *G* against the frequencies for different embroidered stitches for E-clothes
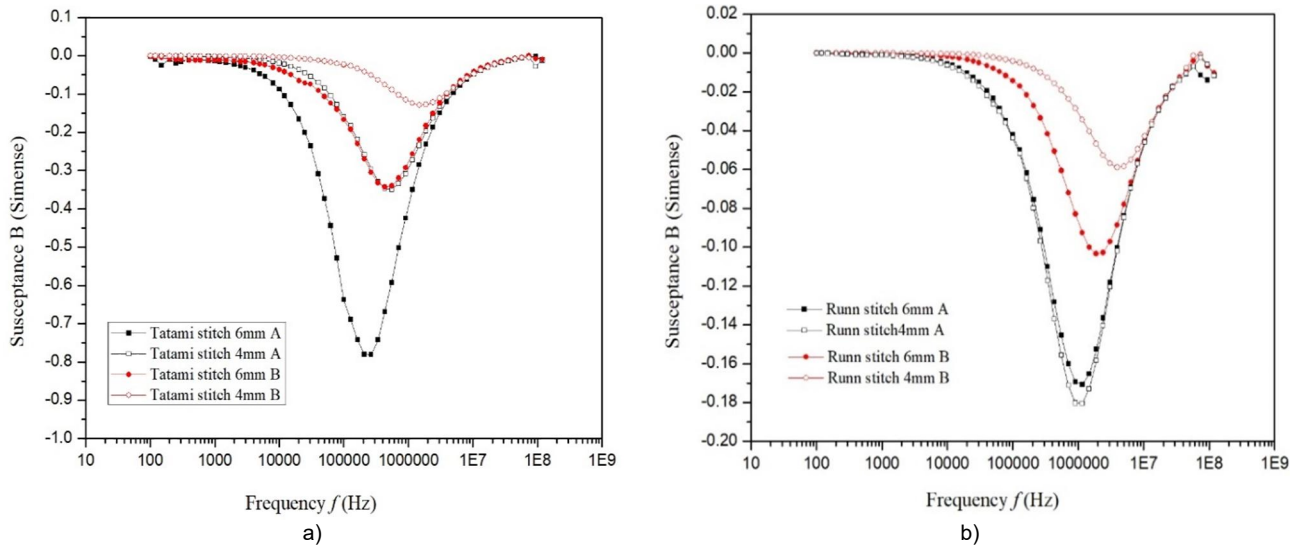
The susceptance *B* of this conductive thread has much higher values than B. This mean the energy stored in the stitches is much higher and it has followed the behavior and trend of both impedance |*Z*| and admittance |*Y*| against frequencies. In Figure 16, the Tatami 6 mm has susceptance *B* at -0.8 S at 265 KHz, Tatami 4 mm both have much close values of *B* at -0.44 S and -0.41 S at 438 KHz and 606 KHz, respectively. The Running stitches in 4 mm and 6 mm stitches have lower susceptance *B* as -0.175 S at 1.06 MHz. There for the real and imaginary component of the complex admittance is illustrated in the Figures 15 and 16. In the Figure 16, the conductance *G* is behaving as similar as the admittance but in different values and stability against the frequency up to 30 MHz. All conductance located in between 0.1-1 S approximately all over the measured frequency range. Then, the instability in the conductance after 30 MHz is due to the resonance of the silver metal that is coating the polymeric thread and filament to consist of the used conductive thread in the stitches as the experimental limitations. The imaginary part B which is representing the susceptance *B* of the materials (silvery conductive threads) in embroidered designed shapes by different types of stitches as Tatami, Satin and Running multiplied within two different lengths 4 mm and 6 mm. The susceptance *B* is related to the impedance *Z* and reactance *X* of the materials. Thus, the B can be deduced as the following:

$$Y = G + jB = \frac{1}{Z} = \frac{1}{R + jX} =$$

$$= \left(\frac{R}{R^2 + X^2}\right) + j\left(\frac{-X}{R^2 + X^2}\right) \quad (6)$$

$$B = \frac{-X}{R^2 + X^2} = \frac{-X}{|Z|^2} \quad (7)$$

Therefore, the susceptance *B* is recalculated for all stitches types of Tatami and Running and they are represent in the Figure 16. There are clear differences among type of stitches as well as their lengths. The Tatami 6 mm stitches provided high conductance and low impedance. However, the susceptance *B* is very low near to zero at low frequencies until 4 KHz, then the amount of energy stored in the stitches decreased as seen in Figure 17. When AC passes through a component that contains a finite, nonzero susceptance, energy is alternately stored in, and released from, a magnetic field or an electric field. In the case of a magnetic field, the susceptance is inductive. In the case of an electric field, the susceptance is capacitive. Inductive susceptance is assigned negative imaginary number values, and capacitive susceptance is assigned positive imaginary number values. As the inductance of a component increases, its susceptance becomes smaller negatively (that is, it approaches zero from the negative side) in imaginary terms, assuming the frequency is held constant. As the frequency increases for a given value of inductance, the same thing happens. Therefore, in case of embroidered stitches all susceptance *B* values are negative and then the released energy would be inductive. The Tatami stitches with 6 mm length have stored much energy at high frequency 400 KHz as well as Satin 6 mm. However, energy but at higher frequency near to 1 MHz. the Tatami 4 mm is much less than pervious stitches but more shifted to higher frequency 1.5 MHz. Finally, running stitches store much lower energy but higher shift toward high frequencies 2 MHz and 6 MHz for Running 6 mm and Running 4 mm stitches.

Figure 17 The semi-log scale plot of the imaginary part of admittance *Y* as the susceptance B against the frequencies for different embroidered stitches for E-clothes

4 CONCLUSION

The conductive threads are very crucial and essential parts of smart textiles but there is a lack of information in general about the operating parameters of embroidery with conductive threads and their influences on communication among electronic components in the e-textiles product. In this article, silver-coated conductive threads have been employed in the fabrication of 4 embroidered designs with two different stitch types (Tatami, Running) and two lengths for each stitch (4 mm, 6 mm).

The influences of embroidery parameters and factors such as length of stitches as well as the type of stitches were investigated against the electrical properties of each design for each conductive thread usage.

Microstructure properties of conductive threads were characterized by energy-dispersive X-ray (EDX) and scanning electron microscopy (SEM). The embroidery process was done by the computerized embroidery machine. The effects of embroidery parameters such as different stitch type, stitch length and type of thread conductive were evaluated. The electrical characteristics also have been determined for the textile without any embroidered stitches of conductive threads.

The electrical characteristics were measured and determined in the frequency domain from 100 kHz-120 MHz. The impedance and resistivity of threads are determined also using the AC voltages at three different frequencies 100 kHz, 1 MHz and 10 MHz. The applied voltages are from 0.0-1.0 volts through thirty (30) steps.

The alternative current AC measurements were conducted for impedance, phase angle, and their corresponding parameters such as real-valued resistance, reactance, admittance, conductance, susceptance and Nyquist plot of ac impedance. Thus, results can be summarized as follows:

- The phase angle in textile is stable against all frequencies up to 100 MHz at -89° which is the characteristic of good small resistor accompanied with a capacitor. The reason for that is the textile in between parallel two electrodes acting as typical dielectric material.

- All impedance values are located between 0.3 Ω up to 6.18 Ω. Once, the impedance is crossing the frequency of 10 MHz, the polarization of silver is contributing to the measurement so that all stitches types with different lengths have the same behavior and trend.

- The phase angle is increased exponentially from very low values near to zero until 1 MHz, then the angle continues increasing into the plateau that started from 1-10 MHz with values near 90°. This mean the designs shapes by embroidered stitches are acting as perfect resistor at low frequencies while they are acting as perfect inductor at high frequencies.

- The 6 mm stitches length in all stitch types provides low resistance rather than 4 mm stitches against the common prediction. This could be explained as the stress and strain due to the automatic machines of embroidery are less in 6 mm if compared to these stresses accompanied with 4 mm stitches length.

- The reactance *X* is below 1 Ω until 1 MHz, while there is continuous increase after 1 MHz till 100 Ω at 120MHz, approximately. There are no big differences in X for all types of stitches with their different stitch lengths approximately as well as HC12 conductive thread embroidery.

The *X* is a typical trend without any significant differences in all types of stitches with their different stitch lengths. Therefore, these designs of embroidered shapes by certain stitches could be a good potential for antenna applications.

- The Nyquist plot here is typical for conductive component for all stitch types in both stitches' lengths 4 mm and 6 mm. The Nyquist plot of Tatami stitches of 6 mm length is showing the lowest value of impedance overall the frequencies against the lock stitches (B thread) 4 mm length which shows the highest impedance and resistance.

- The absolute admittance |*Y*| values are plotted against the applied frequencies from 100 Hz-120 MHz. The current flow is easily conduced in designed embroidered stitches by Tatami stitches (A thread) as the length parameter 6 mm very easy starting from 3 S to 0.8 S along with frequencies up to 800 kHz. However, the stability of the admittance against the high frequency is in favor to the lock stitches than others stitch types.

- All conductance values of stitch types and lengths located in between 0.35-2.0 S approximately all over the measured frequency range. Then, the instability in the conductance after 30 MHz is due to the resonance of the silver metal that is coating the polymeric thread and filament conductive thread as the experimental limitations.

- The susceptance *B* of the A conductive thread has much higher values than B conductive thread. This means the energy stored in the stitches is much higher and it has followed the behavior and trend of both impedance |*Z*| and admittance |*Y*| against frequencies. The Tatami 6 mm (A thread) has susceptance *B* at -0.8 S at 265 KHz. Therefore, in the case of embroidered stitches all susceptance *B* values are negative and then the released energy would be inductive.

- Therefore, these findings are valuable for fabricating any of embroidered e-textiles such as high-performance circuits, antenna applications and other electrically conductive systems and devices. Additionally, these designs of embroidered shapes by certain stitches could be a good potential for antenna applications.

5   REFERENCES

1. Ismar E., Behadir S.K., Kalaoglu F, Koncar V.: Futuristic clothes: electronic textiles and wearable technologies, Global Challenges 4(2), 2020, pp. 2056-6646, https://doi.org/10.1002/gch2.201900092

2. Mecnika V., Hoerr M., Krievins I., Jockenhoevel S., Gries T.: Technical embroidery for smart textiles, Materials Science. Textile and Clothing Technology 9, 2014, pp. 56-63, DOI: 10.7250/mstct.2014.009

3. Hughes-Riley T., Dias T., Cork C.: A historical review of the development of electronic textiles, Fibers 6(2), 2018, 34 p., https://doi.org/10.3390/fib6020034

4. Mecnika V., Scheulen K., Anderson C.F., et al.: Joining technologies for electronic textiles, chapter 7 in Electronic Textiles: Smart Fabrics and Wearable Technology, Dias T. (Ed.), Elsevier Science , 2015, p. 133-153, DOI: 10.1016/B978-0-08-100201-8.00008-4

5. Aigner R., Pointner A., Preindl T., et al.: Embroidered resistive pressure sensors: A novel approach for textile interfaces, Proceedings of the 2020 CHI Conference on Human Factors in Computing Systems, 2020, 13 p., https://doi.org/10.1145/3313831.3376305

6. ZSK, A guide to technical embroidery. 2020, ZSK, https://catalog.zsk.de/download/CARL-Autumn-2020.pdf

7. Linz T., Vieroth R., Dils C., et al.: Embroidered interconnections and encapsulation for electronics in textiles for wearable electronics applications, Advances in Science and Technology 60, 2008, pp. 85-94, https://doi.org/10.4028/www.scientific.net/AST.60.85

8. Roh J.-S.: Conductive Yarn Embroidered Circuits for System on Textiles, chapter in Wearable Technologies, 2018, pp. 161-175, http://dx.doi.org/10.5772/intechopen.76627

9. Eichhoff J., Hehl A., Jockenhoevel S., Gries T.: Textile fabrication technologies for embedding electronic functions into fibres, yarns and fabrics, chapter 7 in Multidisciplinary Know-How for Smart-Textiles Developers, Woodhead Publishing Series in Textiles, 2013, pp. 191-226, https://doi.org/10.1533/9780857093530.2.191

10. Trindade I.G., Machado da Silva J., Miguel R., et al.: Design and evaluation of novel textile wearable systems for the surveillance of vital signals, Sensors 16(10), 2016, 15 p., https://doi.org/10.3390/s16101573

11. McCann J.: The garment design process for smart clothing: from fibre selection through to product launch, chapter 4 in Smart clothes and Wearable Technology, Woodhead Publishing Series in Textiles 2009, pp. 70-94, https://doi.org/10.1533/9781845695668.1.70

12. Post E.R., Orth M., Russo P.R., et al.: E-broidery: Design and fabrication of textile-based computing, IBM Systems Journal 39(3.4), 2000, pp. 840-860, DOI: 10.1147/sj.393.0840

13. Taylor A.: Digital embroidery techniques for smart clothing, chapter 14 in Smart Clothes and Wearable Technology, Woodhead Publishing Series in Textiles, 2009, pp. 279-299, https://doi.org/10.1533/9781845695668.3.279

14. Rho S., Lim D., Yoo E., Hwang E.: The study on Seebeck effect of textile thermocouple manufactured by embroidery technique, Proceedings of the 19th World Textile Conference on Textiles at the Crossroads - AUTEX2019, Ghent, Belgium, 11-15 June 2019, pp. 1-3

15. Agcayazi T., Chatterjee K., Bozkurt A., Ghosh T.K.: Flexible interconnects for electronic textiles, Advanced Materials Technologies 3(10), 2018, art. No. 1700277, https://doi.org/10.1002/admt.201700277

16. Linz T., Kallmayer C., Aschenbrenner R., et al.: Fully untegrated EKG shirt based on embroidered electrical interconnections with conductive yarn and miniaturized flexible electronics, International Workshop on Wearable and Implantable Body Sensor Networks (BSN'06), IEEE, 2006, DOI: 10.1109/BSN.2006.26

17. Shafti A., Ribas Manero R.B., Borg A.M., et al.: Embroidered electromyography: A systematic design guide. IEEE Transactions on Neural Systems and Rehabilitation Engineering 25(9), 2016, pp. 1472-1480, DOI: 10.1109/TNSRE.2016.2633506

18. Lee S., Jamil B., Kim S., Choi Y.: Fabric vest socket with embroidered electrodes for control of myoelectric prosthesis, Sensors 20(4), 2020, pp. 1-17, https://doi.org/10.3390/s20041196

19. Linz T., Gourmelon L., Langereis G.: Contactless EMG sensors embroidered onto textile, Proceedings of the 4th International Workshop on Wearable and Implantable Body Sensor Networks (BSN 2007), IFMBE Proceedings 13. Springer, Berlin, Heidelberg, 2007, pp. 29-34, https://doi.org/10.1007/978-3-540-70994-7_5

20. Roh J.-S., Kim S.: All-fabric intelligent temperature regulation system for smart clothing applications, Journal of Intelligent Material Systems and Structures 27(9), 2016, pp. 1165-1175, https://doi.org/10.1177/1045389X15585901

21. Tsolis A., Whittow W.G., Alexandridis A.A., et al.: Embroidery and related manufacturing techniques for wearable antennas: challenges and opportunities, Electronics 3(2), 2014, pp. 314-338, https://doi.org/10.3390/electronics3020314

22. Zhang S.: Design advances of embroidered fabric antennas, Loughborough University, 2014,

23. Acti T., Chauraya A., Zhang S., et al.: Embroidered wire dipole antennas using novel copper yarns, IEEE Antennas and Wireless Propagation Letters 14, 2015, pp. 638-641, DOI: 10.1109/LAWP.2014.2371338

24. Ouyang Y., Chappell W.J.: High frequency properties of electro-textiles for wearable antenna applications, IEEE Transactions on Antennas and Propagation 56(2), 2008, pp. 381-389, DOI: 10.1109/TAP.2007.915435

25. Linz T., Simon E.P., Walter H.: Modeling embroidered contacts for electronics in textiles, The Journal of The Textile Institute 103(6), 2012, pp. 644-653, https://doi.org/10.1080/00405000.2011.597568

26. Roh J.-S., Chi Y.-S., Lee J.-H., et al.: Characterization of embroidered inductors, Smart Materials and Structures 19(11), 2010, 12 p., https://doi.org/10.1088/0964-1726/19/11/115020

27. Gehrke I., Tenner V., Lutz V., et al.: Smart textiles production: Overview of materials, sensor and production technologies for industrial smart textiles, MDPI Books, 2019, 204 p., https://doi.org/10.3390/books978-3-03897-498-7

28. Holleis P., Schmidt P., et al.: Evaluating capacitive touch input on clothes, in Proceedings of the 10th International Conference on Human Computer Interaction with Mobile Devices and Services, 2008, pp. 81-90, https://doi.org/10.1145/1409240.1409250

29. Kindermann P.: Embroidered touchpad sensors, Thesis, Computer Science Department, RWTH Aachen University, 2018, 35 p.

30. Ojuroye O.O., Torah R.N., Komolafe A.O., et al.: Embedded capacitive proximity and touch sensing flexible circuit system for electronic textile and wearable systems, IEEE Sensors Journal 19(16), 2019, pp. 6975-6985, DOI: 10.1109/JSEN.2019.2911561

31. Roh J.-S., Mann Y., Freed A., Wessel D.: Robust and reliable fabric, piezoresistive multitouch sensing surfaces for musical controllers, in Proceedings of the International Conference on New Interfaces for Musical Expression, 30 May - 1 June 2011, Oslo, Norway, pp. 393-398

32. Roh, J.-S.: Textile touch sensors for wearable and ubiquitous interfaces, Textile Research Journal 84(7), 2014, pp. 739-750, https://doi.org/10.1177/0040517513503733

33. Ismar E., Tao X., Rault F, et al.: Towards embroidered circuit board from conductive yarns for E-textiles, IEEE Access 8, 2020, pp. 155329-155336, https://doi.org/10.1109/ACCESS.2020.3018759

34. Gilliland S., Komor N., Starner T., Zeagler C.: The textile interface swatchbook: Creating graphical user interface-like widgets with conductive embroidery, in International Symposium on Wearable Computers (ISWC) 2010, IEEE, 2010, pp. 1-8, https://doi.org/10.1109/ISWC.2010.5665876

35. SASO-ISO-2062:2009. Standard specification for determination of single-end breaking force and elongation at break using constant rate of extension (CRE) tester. Textiles - Yarns from packages. Retrieved from: https://wasif.saso.gov.sa/Pages/User/SearchResults.aspx?searchkey=2062

36. SASO-ISO-2060:1994. Standard specification for determination of linear density (mass per unit length) by the skein method. Textiles - Yarn from packages. Retrieved from: https://wasif.saso.gov.sa/Pages/User/SearchResults.aspx?searchkey=2060

37. SASO-ISO-7211-1:1984. Standard specification for Part 1: Methods for the presentation of a weave diagram and plans for drafting, denting and lifting. Woven fabrics - Construction - Methods of analysis. Retrieved from: https://wasif.saso.gov.sa/Pages/User/SearchResults.aspx?searchkey=7211

38. SASO-ISO-2286-3:1998. Standard specification for Determination of roll characteristics – Part 3: Method for determination of thickness. Rubber- or plastics-coated fabrics. Retrieved from:

https://wasif.saso.gov.sa/Pages/User/SearchResults.aspx?searchkey=2286

39. SASO-GSO-1269:2006. Standard specification for determination of number of threads in woven fabrics. Retrieved from: https://wasif.saso.gov.sa/Pages/User/StandardInfo.aspx?ref=xc354345XS53x4_28237x6yty34554sfswet

40. SASO-ISO-13934-1:2013. Standard specification for determination of maximum force and elongation at maximum force using the strip method. Textiles -- Tensile properties of fabrics. Retrieved from: https://wasif.saso.gov.sa/Pages/User/SearchResults.aspx?searchkey=13934

41. SASO-ISO-3801:1977. Standard specification for determination of mass per unit length and mass per unit area. Textiles - Woven fabrics. Retrieved from https://wasif.saso.gov.sa/Pages/User/SearchResults.aspx?searchkey=3801

42. Bogatin E.: Signal Integrity: Simplified, 1st ed., Prentice Hall Professional, 2003, 587 p., ISBN: 0130669466

43. Halliday D., Resnick R., Walker J.: Fundamentals of Physics, 10th ed., John Wiley & Sons, 2013, 1448 p., ISBN: 978-1-118-23072-5

44. Swielam E., Eltopshy S., Sobhy S.K., et al.: Impact of the fabrication parameters on the performance of embroidered E-clothes, Egyptian Journal of Chemistry 62(1), 2019, pp. 109-117, DOI: 10.21608/ejchem.2018.4555.1399

45. Nassar A., Taha A.S., Labeeb A., Gouda E.S.A.: Structure and properties of the Al-Sn-Cu bearing alloy under different cold rolling conditions, Journal of Materials Science and Engineering B 5(7-8), 2015, pp. 298-304, https://doi.org/10.17265/2161-6221/2015.7-8.007

46. Labeeb A.M., Sobhy S.K., Eltopshy S.M., et al.: Embroidery on textiles as a smart solution for wearable applications, International Design Journal 9(2), 2019, pp. 53-58, DOI: 10.21608/idj.2019.83296

47. Batoo K.M., Kumar S., Lee C.G., Alimuddin: Study of ac impedance spectroscopy of Al doped MnFe2−2xAl2xO4, Journal of Alloys and Compounds 480(2), 2009, pp. 596-602, https://doi.org/10.1016/j.jallcom.2009.01.137

48. Negroiu R., Svasta P., Ionescu C., Vasile A.: Investigation of supercapacitor's impedance based on spectroscopic measurements, in 1st PCNS Passive Components Networking Days, Brno, Czech Republic, 12-15th Sept. 2017

49. Abbasi A., Hosseini S., Somwangthanaroj A., et al.: Poly (2, 6-dimethyl-1, 4-phenylene oxide)-based hydroxide exchange separator membranes for zinc–air battery, International Journal of Molecular Sciences 20(15), 2019, pp. 1-17, https://doi.org/10.3390/ijms20153678